Power Value Development for Smart Households with Multilevel-THSeAF and PR Controller

Akkemi Suryaprakash Reddy[1], Md. Faizullah[2]

[1]PG Scholar, Dept. of EEE, Dr.K.V. Subba Reddy Institute of Technology, Kurnool, A.P.

[2]Assistant Professor, Dept. of EEE, Dr.K.V. Subba Reddy Institute of Technology, Kurnool, A.P.

ABSTRACT: In this paper, a transformerless hybrid series active filter using a sliding-mode control algorithm and a notch harmonic detection technique are implemented on a single-phase distribution feeder. This method provides compensation for source current harmonics coming from a voltage fed type of nonlinear load (VSC) and reactive power regulation of a residential consumer. The realized active power filter enhances the power quality while cleaning the point of common coupling (PCC) from possible voltage distortions, sags, and swells initiated through the grid. Furthermore, to overcome drawbacks of real-time control delay, a computational delay compensation method, which accurately generates reference voltages, is proposed. Based on an improved compensation strategy, while the grid current remains clean even with a small compensation gain, voltage disturbances initiated by the power system are obstructed by the compensator, and the PCC became free of voltage harmonics and protected from sag and swell. Simulation results are presented and discussed.

Index Terms—Active rectifier, current harmonics, hybrid series active filter, power quality, real-time sliding-mode control (SMC).

I. INTRODUCTIN :

THE forecast of future Smart Grids associated with electric vehicle charging stations has created a serious concern on all aspects of power quality of the power system, while widespread electric vehicle battery charging units have detrimental effects on power distribution system harmonic voltage level. On the other hand, the growth of harmonics fed from nonlinear loads like electric vehicle propulsion battery chargers which indeed have detrimental impacts on the power system and affect plant equipment, should be considered in the development of modern grids. Likewise, the increased rms and peak value of the distorted current waveforms increase heating and losses and cause the failure of the electrical equipment. Such phenomenon effectively reduces system efficiency and should have properly been addressed.

Moreover, to protect the point of common coupling (PCC) from voltage distortions, using a dynamic voltage restorer (DVR) function is advised. A solution is to reduce the pollution of power electronics-based loads directly at their source. Although several attempts are made for a specific case study, a generic solution is to be explored. There exist two types of active power devices to overcome the described power quality issues. The first category are series active filters (SeAFs), including hybrid-type ones. They were developed to eliminate current harmonics produced by nonlinear load from the power system. SeAFs are less scattered than the shunt type of active filters . The advantage of the SeAF compared to the shunt type is the inferior rating of the compensator versus the load nominal rating . However, the complexity of the configuration and necessity of an isolation series

transformer had decelerated their industrial application in the distribution system. The second category was developed in concern of addressing voltage issues on sensitive loads. Commonly known as DVR, they have a similar configuration as the SeAF. These two categories are different from each other in their control principle. This difference relies on the purpose of their application in the system. The hybrid series active filter (HSeAF) was proposed to address the aforementioned issues with only one combination. Hypothetically, they are capable to compensate current harmonics, ensuring a power factor (PF) correction and eliminating voltage distortions at the PCC . These properties make it an appropriate candidate for power quality investments.

The three-phase SeAFs are well documented, whereas limited research works reported the single-phase applications of SeAFs in the literature. In this paper, a single-phase transformerless HSeAF is proposed and capable of cleaning up the grid-side connection bus bar from current harmonics generated by a nonlinear load . With a smaller rating up to 10%, it could easily replace the shunt active filter . Furthermore, it could restore a sinusoidal voltage at the load PCC. The advantage of the proposed configuration is that nonlinear harmonic voltage and current producing loads could be effectively compensated. The transformerless hybrid series active filter (THSeAF) is an alternative option to conventional power transferring converters in distributed generation systems with high penetration of renewable energy sources, where each phase can be controlled separately and could be operated independently of other phases. This paper shows that the separation of a three-phase converter into single-phase Hbridge converters has allowed the elimination of the costly isolation transformer and promotes industrial application for filtering purposes. The

setup has shown great ability to perform requested compensating tasks for the correction of current and voltage distortions, PF correction, and voltage restoration on the load terminal.

This paper is organized as follows. The system architecture is introduced in the following section. Then, the operation principle of the proposed configuration is explained. The third section is dedicated to the modeling and analysis of the control algorithm implemented in this work. The dc voltage regulation and its considerations are briefly explained, and the voltage and current harmonic detection method is explicitly described. To evaluate the configuration and the control approach, some scenarios are simulated. Experimental results performed in the laboratory are demonstrated to validate simulations.
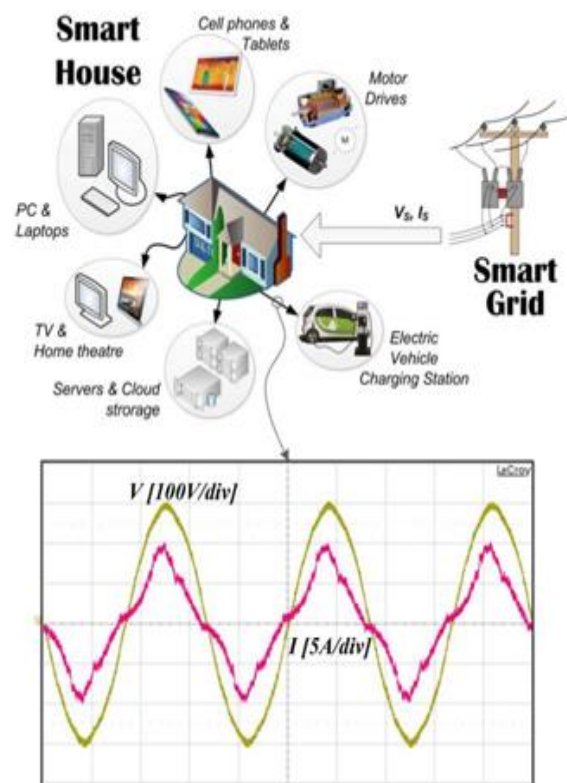
Fig1: Typical residential consumer with electronic loads, and measured electric car (Nissan Leaf) voltage and current patterns connected to a level-2 ac charging station, and an iPhone 4s charger.

This paper is summarized with a conclusion and appendix where further mathematical developments are demonstrated.

II. SYSTEM ARCHITECTURE

A.   System configuration

The compensator represented in Fig. two consists of a construction single-phase convertor connected serial between the utility and also the house's entrance connected terminals. The transformerless hybrid series active filter consists of a five-level office convertor [17] represented in Fig. 3, connected serial between the utility and also the entrance of the building. associate auxiliary provide is connected on the dc aspect. To filter high frequency change harmonics, a passive filter is employed at the output of the convertor. A bank of tuned passive filters ensures an occasional resistivity path for current harmonics. during this paper the studied system is enforced for a rated power of one kVA. to make sure a quick transient response with comfortable stability margins over a good vary of dynamic operations, the controller is enforced on associate Opal- RT/Wanda period of time machine. For associate correct period of time mensuration of electrical variables, the Opal- RT OP8665 probes square measure activity the mensuration task. The system parameters square measure known in Table

I. A variable supply up to a hundred and twenty Vrms is connected to a one kVA non-linear load. The THSeAF is connected serial so as to inject the compensating voltage. On the DC aspect of the compensator, associate auxiliary dc-link energy storage system is put in. Similar parameters also are applied for simulations. a

quick electrical vehicle charging plug level-2 is in addition connected to the load's PCC. The active compensator's office convertor structure is represented in Fig. 3.
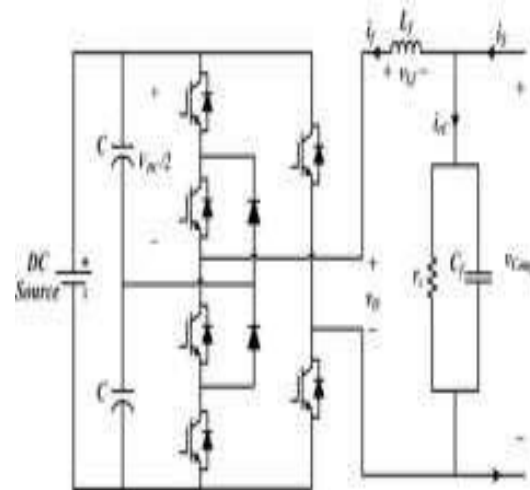

Fig. 2. Hybrid converter topology for the proposed series compensator.

On the DC side of the compensator, auxiliary dc-link energy storage components are installed at a reduced voltage level of 100V. The objective is to propose an efficient device capable of rectifying current related issues in smart grids which also provide sustainable and reliable voltage supply at the point of common coupling that define the entrance of residential or commercial buildings.

Using the circuit of Fig. 2 showing the block diagram and model of equivalent house circuit connection with utility meters and Multilevel-THSeAF connected in series, several critical scenarios such as grid distortion, sag or swell are simulated using discrete time steps of $40\mu s$.

TABLE I

CONFIGURATION PARAMETERS

International Journal of Research

Available at https://edupediapublications.org/journals

e-ISSN: 2348-6848
p-ISSN: 2348-795X
Volume 05 Issue 23
December 2018

Symbol	Definition	Value
V_S	Line phase-to-neutral voltage	110 Vrms
f	System frequency	60 Hz
L_S	Supply equivalent inductance	150 μH*
R, L	Non-linear CSC load	25 Ω, 20mH
Lf	Switching ripple filter inductance	2.5 mH
Cf	Switching ripple filter capacitance	2 μF
r_C	Switching ripple damping resistor	60 Ω
T_S	Opal-RT Synchronous sampling time	40 μs
f_{PWM}	PWM frequency	8 kHz
F_5	Fifth order shunt passive filter	56μF, 5mH
F_7	Seventh order passive filter	14μF, 10mH
F_{11}	Eleventh order passive filter	6μF, 10mH
F_{HPF}	High-pass filter	2μF
K_P, K_r	Controller proportional and resonant gains	2.5, 10
ω_C	Cutoff frequency	5 rad/s
V_{DC}	dc auxiliary power supply voltage	110 V, 120 V*

* Adopted value for the simulation analysis

Table 1

The Multilevel- THSeAF connected in series injects a compensating voltage which results in a drastic improvement of source current distortions and a cleaned load voltage. While the load current contains a THDIL of 12%, the source current is cleaned with a THDIS of 2.1%. When the utility is highly polluted with a THDVS of 25.5%, the load voltage is regulated and contains a THD of only 1.2%.

B. Operation principle

A current fed type of non-linear load could be modeled as a harmonic voltage source in series with an impedance $Z_{Non-Linear}$ or by its Norton equivalent modeled with a harmonic current source in parallel to the impedance. Thévenin's model and Norton's equivalent circuit are depicted in Fig. 4. In this paper the common Norton's equivalent is chosen to follow major related papers. In this work the approach to achieve optimal behavior during the time the grid is perturbed is implemented on the controller [18]. The use of a passive filter is mandatory to compensate current issues and maintaining a constant voltage free of distortions at the load terminals. The non-linear load is modeled by a resistance representing the active power consumed and a current source generating harmonic current. Accordingly, the

impedance Z_L is the equivalent of the nonlinear ($Z_{Non-linear}$) and the linear load (Z_{RL}). The Series active filter, whose output voltage V_{comp} is considered as an ideal controlled voltage source is generating a voltage based on the detecting source current, load voltage, and also the source voltage to achieve optimal results as of (4). This established hybrid approach gives good result and is quite less sensitive to the value of the gain **G** to achieve low levels of current harmonics. The gain **G** is proportional to the current harmonics (I_{sh}) flowing to the grid. Assuming a non-ideal grid supplying feeder voltage that contains important numbers of voltage distortions (V_{Sh}), the equivalent circuit for the fundamental and harmonics are:

$$VS = VS1 + Vsh \qquad (1)$$

$$VL = VL1 + VLh = ZL$$

$$IZ = ZL(IS - Ih) \qquad (2)$$

$$IS = IS1 + ISh = IZ + Ih \qquad (3)$$

$$Vcomp = +GIsh - VLh + Vsh \qquad (4)$$

Where IZ represents the load current in ZL shown in Fig. 6. Using the Kirchhoff's law the following equation is depicted for both the fundamental and harmonics.

$$V_S = Z_S I_S + V_{Comp} + V_L \qquad (5)$$

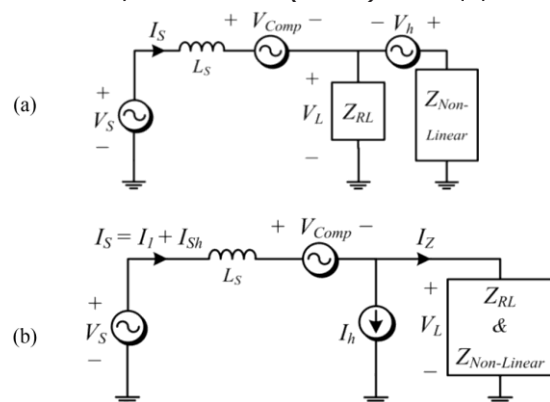$$V_{L1} = Z_L I_{S1}, \qquad V_{Lh} = Z_L(I_{Sh} - I_h) \qquad (6)$$

Fig. 3. Single-phase equivalent phasor model for VSC type of loads, (a) Thévenin's model, (b) Norton equivalent.

By substituting the fundamental of (6) in (5), the source current at fundamental frequency is obtained.

$$I_{S1} = \frac{V_{S1}}{Z_S + Z_L} \qquad (7)$$

(a)

(b)

Fig. 4. Single-phase equivalent phasor model for VSC type of loads, (a) Thévenin's model, (b) Norton equivalent.
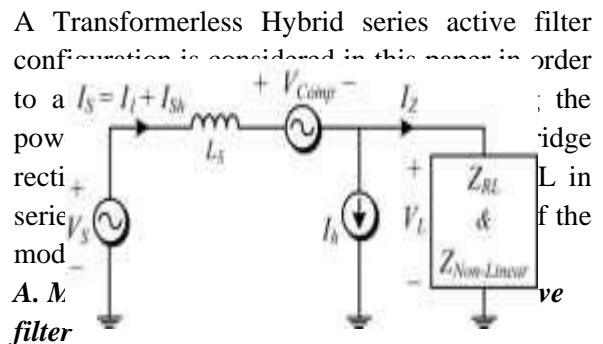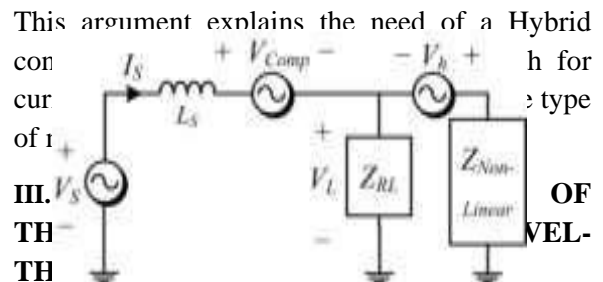
By substituting (4) in (5) for the harmonic components, the harmonic source current is reached as follow.

$$V_{Sh} = Z_S I_{Sh} + G I_{Sh} - V_{Lh} + V_{Sh} + V_{Lh} \rightarrow I_{Sh} = 0 \qquad (8)$$

By introducing (8) into the harmonic component of the load PCC voltage (6), following equation is achieved.

$$V_{Lh} = -Z_L I_h \qquad (9)$$

Consequently in this approach even in presence of source voltage distortions the source current is always clean of any harmonic component. To some extent in this approach the filter behaves as high impedance likewise an open circuit for current harmonics, while the shunt high pass filter tuned at the system frequency, could create a low-impedance path for all harmonics and open circuit for the fundamental component. This argument explains the need of a Hybrid con̲ h for cur̲ type of ̲

III. ̲ OF TH̲ VEL-TH̲

A Transformerless Hybrid series active filter configuration is considered in this paper in order to a̲ the pow̲ idge recti̲ L in serie̲ f the mod̲

A. M̲ ve filter

According to Fig. 3, and the average equivalent circuit of an inverter developed in [19], the small-signal model of the proposed configuration can be obtained. Kirchhoff's rules for voltages and currents, as applied to this system, provide us with the differential equations.

Thereafter, d is the duty cycle of the upper switch of the inverter developed in [19], the small-signal model of the proposed configuration can be obtained. Kirchhoff's rules for voltages and currents, as applied to this system, provide us with the differential equations.

Thereafter, d is the duty cycle of the upper switch of the converter leg in a switching period, whereas v and ι denotes the average value in a switching period of the voltage and current of the

same leg. The mean converter output voltage and current are expressed by (10) and (11) as follows.

$$\bar{v}_O = \left(\underbrace{2d-1}_{m}\right) V_{DC} \qquad (10)$$
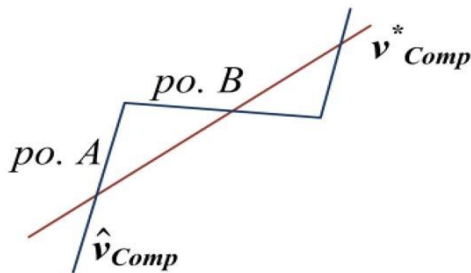
$$\bar{i}_{DC} = m\bar{i}_f \qquad (11)$$

Fig. 5. Compensating voltage versus the reference signal.

According to the scheme on Fig. 3, the arbitrary direction of i_f is chosen to go out from the H-bridge converter. For dynamic studies the accurate model is considered.

$$mV_{DC} = L_f \frac{di_f}{dt} + v_{Comp} \qquad (12)$$

$$r_C C_f \frac{dv_{Comp}}{dt} = -v_{Comp} + r_C(i_f + i_S) \qquad (13)$$

The state-space small-signal ac model could be derived by a linearized perturbation of averaged model as follow:

$$\dot{x} = Ax + Bu \qquad (14)$$

Hence we obtain:

$$\frac{d}{dt}\begin{bmatrix} \bar{i}_f \\ \bar{v}_{Comp} \end{bmatrix} = \begin{bmatrix} 0 & -\frac{1}{L_f} \\ \frac{1}{C_f} & -\frac{1}{r_C C_f} \end{bmatrix} \times \begin{bmatrix} \bar{i}_f \\ \bar{v}_{Comp} \end{bmatrix}$$

$$+ \begin{bmatrix} \frac{V_{DC}}{L_f} & 0 \\ 0 & \frac{1}{C_f} \end{bmatrix} \times \begin{bmatrix} m \\ i_S \end{bmatrix}. \qquad (15)$$

The output vector is then

$$Y = cx + Du \qquad (16)$$

or

$$y = \begin{bmatrix} 0 & 1 \end{bmatrix} \times \begin{bmatrix} \bar{i}_f \\ \bar{v}_{Comp} \end{bmatrix} \qquad (17)$$

By means of (15) and (17), the state-space representation of the model could be obtained. The second order relation between the compensating voltage and the duty cycle could be reached as follows.

$$C_f \frac{d^2 v_{Comp}}{dt^2} + \frac{1}{r_C} \frac{dv_{Comp}}{dt} + \frac{1}{L_f} v_{Comp} = \frac{V_{DC}}{L_f} m + \frac{di_S}{dt} \qquad (18)$$

This model could then be used in developing the converter's controller and its stability analysis.

IV. CONTROL ALGORITHM OF THE SYSTEM

The Multilevel Transformerless Hybrid series active filter configuration considered in this work is taking advantage of an NPC converter to reduce passive components rating while, delivering a high-quality compensating voltage. The controller strategy implemented in this paper is based on a Proportional plus resonant controller to generate IGBT's gate signals. The reference signal applied to the P+R regulator is created by two detection block taking care of the voltage and current issues respectively as presented in the following control diagram.
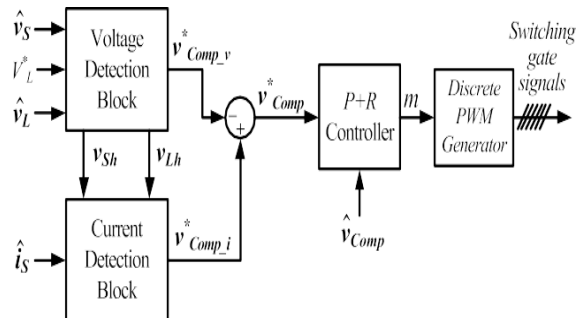
Fig. 6. Control system architecture scheme for P+R.

In this Rapid Control Prototyping (RCP) application, the whole controller is implemented on the Opal-RT device, where the controller is run on a fixed time step size determined in the core of the paper in Table I. The inputs of the controller described in Fig. 8, are measured using the Opal-RT probes. The output signals of the controller are the switching gate signals produced over the digital output of the real-time simulator. These signals are then passing through opt isolator board to enable semiconductor gate driver's control.

As the compensating voltage reference is an oscillating signal with several harmonic components, the P+R regulator has numerous advantages over other control approaches. To develop the controller, the average equivalent circuit of the converter is used with the small-signal model of the proposed configuration to analyze the effects of delays on the transient response of the compensator. The proposed control strategy takes advantages of both a proportional and resonant controller to generate gating signals.

The transfer function of the controller with a multi-resonant property is given by:

$$G_{P-R}(s) = K_P + \sum_{h=1,3,5,7,...}^{n} \frac{2K_{rh} \cdot \omega_C \cdot s}{s^2 + 2\omega_C \cdot s + (h \cdot \omega)^2} \quad (19)$$

Where h is the harmonic order, Kp and Krh are gains, and $h\omega$ is the resonant frequency and ωC is the cutoff frequency. Their values are depicted in Table I. The frequency responses with a delay time are depicted in Fig. 9, where the Bode diagram shows the superiority of the PR controller over the system without regulation and with a PI regulator.

To implement the controller on the digital simulator the transfer function should be obtained by discretization via numerical integration. To obtain the discrete equivalent of a transfer function via numerical integration, one should apply appropriate numerical integration techniques depending on the sensitivity and stability requirements to the system differential equation [20].
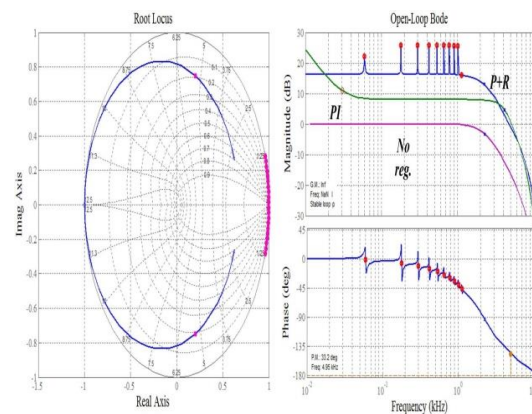

Fig. 7. Frequency response of the system with a 40 μs delay time; using the PI controller, P+R controller, and with a closed-loop controller. (a) Root Locus diagram. (b) Bode diagram.

The P+R controller function is then calculated, where z is the variable in the z-domain and T is the sampling time constant also known as step-time TS in Matlab environment. By performing the Z-transform, using the Tustin or bilinear approximation based on the trapezoidal rule, on (19), the discrete transfer function is achieved as follow. The frequency variable "s" is replaced by the following term.

$$s \rightarrow \frac{2 \cdot (z-1)}{T(z+1)}, \quad s^2 \rightarrow \frac{4(z-1)^2}{T^2(z+1)} \quad (20)$$

This results in the following discrete transfer function in the z-domain.

According to the two developed discrete function, one can implement either of them for a real-time simulation or a practical experiment on

a digital controller. Meanwhile, the choice of gains is tied with the stability study of the transfer

$$
\begin{aligned}
&G_{P+R}(z) \\
&= K_P + \sum_{h=1,3,5,7,\ldots}^{n} \frac{2K_{rh} \cdot \omega_C \cdot z^2 \cdot T - K_{rh} \cdot \omega_C \cdot T}{\left(1 + \omega_C T + (h\omega T)^2\right)z^2 + \left(\frac{(h\omega T)^2}{2} - 2\right)z + 1 - \omega_C T + \frac{(h\omega T)^2}{4}}
\end{aligned}
\tag{21}
$$

According to the two developed discrete function, one can implement either of them for a real-time simulation or a practical experiment on a digital controller. Meanwhile, the choice of gains is tied with the stability study of the transfer function. The gains should be chosen depending on the sampling time imposed by the digital controller, and the behavior of the system itself. In a general rule; the more the sampling time T, has a smaller value, the more the chance to reach a stable system is observed.
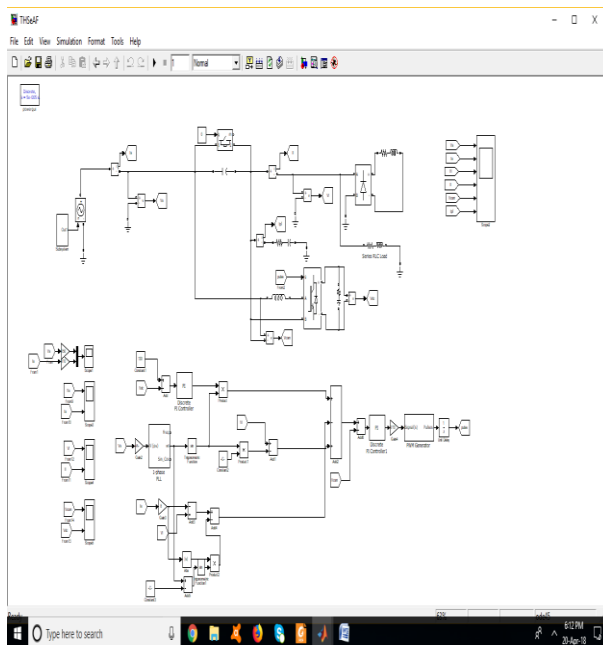
V. SIMULATION RESULTS

Fig 8: Proposed simulation diagram

The proposed THSeAF configuration was simulated in MATLAB/simulink using the discrete time of Ts=10µs.The combination of a single-phase nonlinear load and linear load with a rated power of 2kVA with a 0.74 lagging 120Vrms 60Hz variable source is used. THSeAF connected in series to the system compensates the current harmonics and voltage distortions. A gain G = 8Ω (=1.9 p.u) was used to control current harmonics. During the grid's voltage distortion, the compensator regulates the load voltage magnitude, compensates the current harmonics and corrects the PF. The load voltage VL THD is 0.44%, while the source voltage is highly distorted (THDVs = 1.45%).
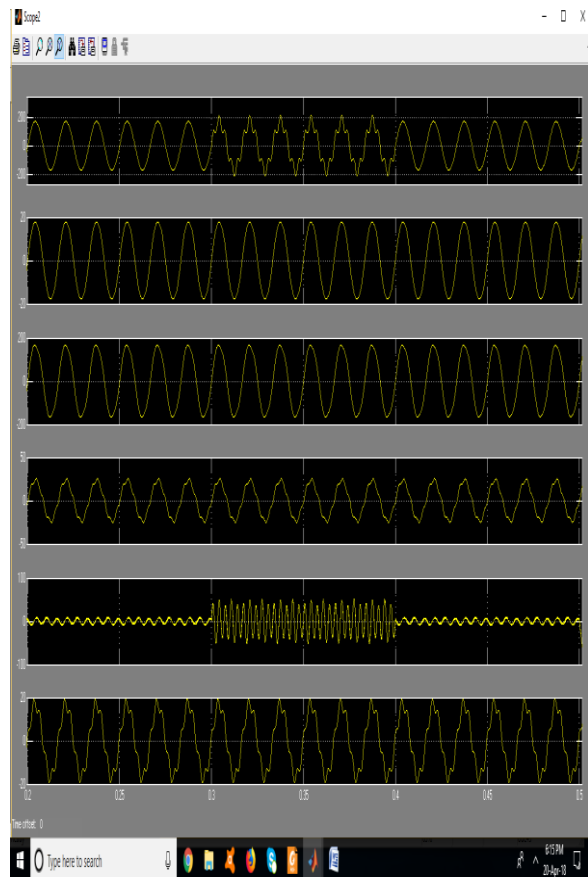

Fig. 9. Compensating current harmonics and voltage regulation, during grid initiated distortions. (a) Source voltage *vS*, (b) source

current *iS*, (c) load voltage *vL*, (d) load current *iL*, (e) active-filter voltage *VComp*, (f) Harmonics current of the passive filter *iPF*, (g) Converter's output voltage *VOut*.
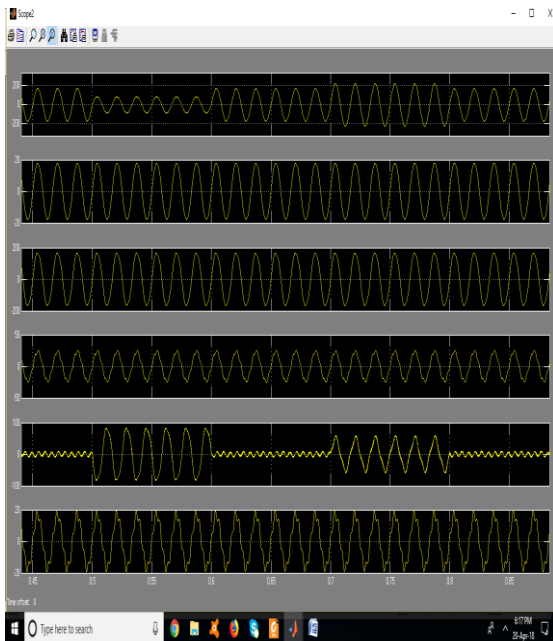

Fig. 10. System response during grid sags and swells. (a) Source voltage *vS*, (b) source current *iS*, (c) load voltage *vL*, (d) load current *iL*, (e) active-filter voltage *VComp*, (f) Harmonics current of the passive filter *iPF*, (g) Converter's output voltage *VOut*
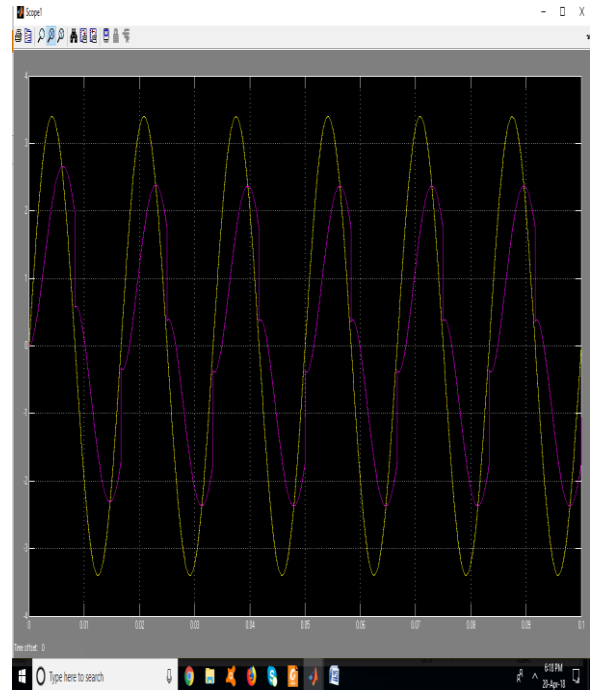

Fig. 11. Typical modern residential consumer with non-linear electronic loads and a Nissan LEAF measured voltage and current waveforms plugged to a level-2 charging station.

The grid is cleaned of current harmonics with a unity power factor (UPF) operation, and the THD is reduced to less than 1% in normal operation and less than 4% during grid perturbation. While the series controlled source cleans the current of harmonic components, the source current is forced to be in phase with the source voltage. The series compensator has the ability to slide the load voltage in order for the PF to reach unity. Furthermore, the series compensator could control the power flow between two PCCs. The compensator shows high efficiency in normal operation where the total compensator losses including switching, inductor resistances, and damping resistances are equal to 44 W which is less than 2.5% of the system rated power. While cleaning the source

current from harmonics and correcting the PF, the compensator regulates the load terminal voltage.

VI. CONCLUSION

In this document, a novel THSeAF configuration with a slidingmode controller was proposed and tested to overcome power quality issues of a voltage fed type of nonlinear load. The theoretical modeling has been realized and simulated for further developments. A second-order SMC is developed and adapted for practical real-time implementations. A notch harmonic detection is implemented and tested to extract harmonic components of a polluted signal. The stability of the controller is also described and analyzed using Lyaponov criteria. It has been demonstrated that the proposed configuration along with the control approach is able to feature reactive power exchange with the utility as well. With regard to the control approach and taking advantage of the proposed robust structure, a harmonic-free voltage is delivered across the residential terminals. The whole system is implemented on a real-time simulator to ensure feasibility of the developed controller. It is worthy to mention that this topology does not make use of a bulky transformer, which is mandatory for series active/hybrid filters topologies; it has a natural feature of limiting short-circuit current during faulty condition. It also replaces the function of UPS/UPQC devices with much less reactive and semiconductor components. Results of the laboratory implementation have demonstrated that this active compensator responds to abrupt variations in the grid voltage by providing a constant and distortion-free supply to the load while eliminating grid current harmonics contributing to the improvement of the grid's power quality.

VII. REFERENCES

[1] L. Jun-Young and C. Hyung-Jun, "6.6-kW onboard charger design using DCM PFC converter with harmonic modulation technique and two-stage dc/dc converter," IEEE Trans. Ind. Electron., vol. 61, no. 3, pp. 1243– 1252, Mar. 2014.

[2] R. Seung-Hee, K. Dong-Hee, K. Min-Jung, K. Jong-Soo, and L. ByoungKuk, "Adjustable frequency duty-cycle hybrid control strategy for fullbridge series resonant converters in electric vehicle chargers," IEEE Trans. Ind. Electron., vol. 61, no. 10, pp. 5354–5362, Oct. 2014.

[3] P. T. Staats, W. M. Grady, A. Arapostathis, and R. S. Thallam, "A statistical analysis of the effect of electric vehicle battery charging on distribution system harmonic voltages," IEEE Trans. Power Del., vol. 13, no. 2, pp. 640–646, Apr. 1998.

[4] A. Kuperman, U. Levy, J. Goren, A. Zafransky, and A. Savernin, "Battery charger for electric vehicle traction battery switch station," IEEE Trans. Ind. Electron., vol. 60, no. 12, pp. 5391–5399, Dec. 2013.

[5] Z. Amjadi and S. S. Williamson, "Modeling, simulation, control of an advanced Luo converter for plug-in hybrid electric vehicle energy-storage system," IEEE Trans. Veh. Technol., vol. 60, no. 1, pp. 64–75, Jan. 2011.

[6] H. Akagi and K. Isozaki, "A hybrid active filter for a three-phase 12-pulse diode rectifier used as the front end of a medium-voltage motor drive," IEEE Trans. Power Del., vol. 27, no. 1, pp. 69–77, Jan. 2012.

[7] A. F. Zobaa, "Optimal multiobjective design of hybrid active power filters considering a distorted environment," IEEE Trans. Ind. Electron., vol. 61, no. 1, pp. 107–114, Jan. 2014.

[8] D. Sixing, L. Jinjun, and L. Jiliang, "Hybrid cascaded H-bridge converter for harmonic current compensation," IEEE Trans. Power

Electron., vol. 28, no. 5, pp. 2170–2179, May 2013.

[9] M. S. Hamad, M. I. Masoud, and B. W. Williams, "Medium-voltage 12-pulse converter: Output voltage harmonic compensation using a series APF," IEEE Trans. Ind. Electron., vol. 61, no. 1, pp. 43–52, Jan. 2014.

[10] J. Liu, S. Dai, Q. Chen, and K. Tao, "Modelling and industrial application of series hybrid active power filter," IET Power Electron., vol. 6, no. 8, pp. 1707–1714, Sep. 2013.

[11] A. Javadi, H. Fortin Blanchette, and K. Al-Haddad, "An advanced control algorithm for series hybrid active filter adopting UPQC behavior," in Proc. 38th Annu. IEEE IECON, Montreal, QC, Canada, 2012, pp. 5318–5323.

[12] O. S. Senturk and A. M. Hava, "Performance enhancement of the singlephase series active filter by employing the load voltage waveform reconstruction and line current sampling delay reduction methods," IEEE Trans. Power Electron., vol. 26, no. 8, pp. 2210–2220, Aug. 2011.

[13] A. Y. Goharrizi, S. H. Hosseini, M. Sabahi, and G. B. Gharehpetian, "Three-phase HFL-DVR with independently controlled phases," IEEE Trans. Power Electron., vol. 27, no. 4, pp. 1706–1718, Apr. 2012.

[14] H. Abu-Rub, M. Malinowski, and K. Al-Haddad, Power Electronics for Renewable Energy Systems, Transportation, Industrial Applications. Chichester, U.K.: Wiley InterScience, 2014.

[15] S. Rahmani, K. Al-Haddad, and H. Kanaan, "A comparative study of shunt hybrid and shunt active power filters for single-phase applications: Simulation and experimental validation," Math. Comput. Simul., vol. 71, no. 4–6, pp. 345–359, Jun. 19, 2006.

[16] W. R. Nogueira Santos et al., "The transformerless single-phase universal active power filter for harmonic and reactive power compensation," IEEE Trans. Power Electron., vol. 29, no. 7, pp. 3563–3572, Jul. 2014.

[17] A. Javadi, H. Fortin Blanchette, and K. Al-Haddad, "A novel transformerless hybrid series active filter," in Proc. 38th Annu. IEEE IECON, Montreal, QC, USA, 2012, pp. 5312–5317.

[18] H. Liqun, X. Jian, O. Hui, Z. Pengju, and Z. Kai, "High-performance indirect current control scheme for railway traction four-quadrant converters," IEEE Trans. Ind. Electron., vol. 61, no. 12, pp. 6645–6654, Dec. 2014.

[19] E. K. K. Sng, S. S. Choi, and D. M. Vilathgamuwa, "Analysis of series compensation and dc-link voltage controls of a transformerless selfcharging dynamic voltage restorer," IEEE Trans. Power Del., vol. 19, no. 3, pp. 1511–1518, Jul. 2004.

[20] H. Fujita and H. Akagi, "A practical approach to harmonic compensation in power systems-series connection of passive and active filters," IEEE Trans. Ind. Appl., vol. 27, no. 6, pp. 1020–1025, Nov./Dec. 1991.

[21] A. Varschavsky, J. Dixon, M. Rotella, and L. Mora, "Cascaded nine-level inverter for hybrid-series active power filter, using industrial controller," IEEE Trans. Ind. Electron., vol. 57, no. 8, pp. 2761–2767, Aug. 2010.

[22] X. P. n. Salmero and S. P. n. Litra, "A control strategy for hybrid power filter to compensate four-wires three-phase systems," IEEE Trans. Power Electron., vol. 25, no. 7, pp. 1923–1931, Jul. 2010.

[23] B. Singh, A. Chandra, and K. Al-Haddad, Power Quality Problems and Mitigation Techniques. Chichester, U.K.: Wiley, 2015.

[24] P. Salmeron and S. P. Litran, "Improvement of the electric power quality using series active and shunt passive filters," IEEE Trans. Power Del., vol. 25, no. 2, pp. 1058–1067, Apr. 2010.

[25] S. Srianthumrong, H. Fujita, and H. Akagi, "Stability analysis of a series active filter integrated with a double-series diode rectifier,"

IEEE Trans. Power Electron., vol. 17, no. 1, pp. 117–124, Jan. 2002.